Angle-Dependent X-Ray Magnetic Circular Dichroism from (Ga,Mn)As: Anisotropy and Identification of Hybridized States

K. W. Edmonds,[1] G. van der Laan,[2] A. A. Freeman,[1,2] N. R. S. Farley,[1,2] T. K. Johal,[2] R. P. Campion,[1] C. T. Foxon,[1] B. L. Gallagher,[1] and E. Arenholz[3]

[1]*School of Physics and Astronomy, University of Nottingham, Nottingham NG7 2RD, United Kingdom*
[2]*CCLRC Daresbury Laboratory, Warrington WA4 4AD, United Kingdom*
[3]*Advanced Light Source, Lawrence Berkeley National Laboratory, Berkeley, California 94720, USA*

(Received 8 November 2005; published 22 March 2006)

Remarkably anisotropic Mn $L_{2,3}$ x-ray magnetic circular dichroism spectra from the ferromagnetic semiconductor (Ga,Mn)As are reported. States with cubic and uniaxial symmetry are distinguished by careful analysis of the angle dependence of the spectra. The multiplet structures with cubic symmetry are qualitatively reproduced by calculations for an atomiclike d^5 configuration in tetrahedral environment, and show zero anisotropy in the orbital and spin moments within the experimental uncertainty. However, hybridization with the host valence bands is reflected by the presence of a preedge feature with a uniaxial anisotropy and a marked dependence on the hole density.

DOI: 10.1103/PhysRevLett.96.117207 PACS numbers: 75.50.Pp, 71.20.Nr, 75.30.Gw, 78.70.Dm

The manipulation of spin in semiconductors is the subject of widespread research because of its relevance to applications in nonvolatile logic and quantum computation. Mn-doped III-V semiconductors such as (Ga,Mn)As [1], in which the transition metal dopant provides both a magnetic moment and a spin-polarized charge carrier, have thus attracted strong interest. Recent developments in identifying and removing compensating defects have led to Curie temperatures T_C in excess of 170 K [2–4]. Also, much progress has been made in developing a phenomenological understanding of key properties such as magnetic anisotropy [5,6]. However, the microscopic picture of magnetism and anisotropy in III-V magnetic semiconductors is still debated [7–9], and it is unclear whether the Mn states are localized as assumed in *p-d* Zener models [7], strongly hybridized with the host valence band, or forming a separate impurity band. This is due in part to the difficulty in calculating the electronic structure of dilute systems with localized *d* states, and in part to conflicting experimental results.

There is growing interest in exploiting x-ray absorption spectroscopy (XAS) and x-ray magnetic circular dichroism (XMCD) as local probes of electronic structure and magnetism in semiconductors [10–16]. Mn $L_{2,3}$ XAS measures the excitation from the Mn $2p$ to $3d$ levels, thus probing the unoccupied valence states with Mn $3d$ character. The XMCD is the difference between XAS spectra obtained with opposite alignments of the sample magnetization and x-ray helicity vector. Integrated intensities together with sum rules can be used for quantitative and element-specific determination of spin and orbital magnetic moments per atom, m_{spin} and m_{orb} [17,18]. Furthermore, angle-dependent XMCD can be used to determine the anisotropy of the moments [19,20], which is fundamentally related to the magnetocrystalline anisotropy [21,22]. Here, we present a detailed study of angle-dependent XMCD from (Ga,Mn)As. Pronounced anisotropies in the multiplet structure are observed, with individual features having either cubic or uniaxial symmetry. The cubic features are shown to be atomiclike, with no net anisotropy in the magnetic moments, and no significant Mn or hole concentration dependence. In contrast, the small uniaxial feature has a systematic dependence on hole density, indicating that this feature corresponds to states close to the Fermi energy. Thus, our angle-dependent XMCD measurements allow the identification of both localized and hybridized Mn *d* states in (Ga,Mn)As.

The Mn $L_{2,3}$ XAS and XMCD measurements are performed on ID8 of the European Synchrotron Radiation Facility, Grenoble, and station 4.0.2 of the Advanced Light Source, Berkeley. The (Ga,Mn)As samples are prepared *ex situ* by low-temperature molecular beam epitaxial growth on GaAs(001) substrates [23]. In some cases, samples were annealed in air at 190 °C after growth, which is a known procedure for increasing the hole density, p, due to outdiffusion of compensating defects [2,3]. To remove surface oxides, the samples are etched in concentrated HCl just prior to loading in the vacuum chamber [12].

The main crystallographic axes are labeled in the inset of Fig. 1(a). Throughout the measurements, the external magnetic field is aligned parallel (or antiparallel) to the x-ray incidence direction. Measurements are made by rotating the sample polar (θ) and azimuthal (ϕ) angles. The measurement axis, defined by the field and x-ray helicity vector, is rotated by θ from the out-of-plane [001] direction, towards either the [010] ($\phi = 0$) or the [110] ($\phi = 45°$) in-plane direction. X-ray absorption spectra are obtained in total-electron-yield mode, reversing the external magnetic field after each spectrum. To improve the signal-to-noise ratio, sets of measurements taken with left and right circularly polarized x rays are averaged. The only

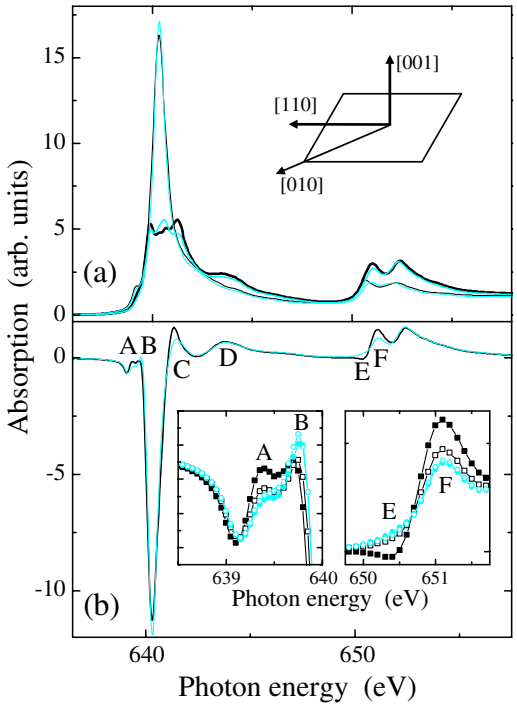

FIG. 1 (color online). (a) Mn $L_{2,3}$ XAS for parallel and antiparallel alignment of helicity and magnetization, for magnetization along [001] (black lines) and [111] (blue or gray lines); (b) XMCD spectra for magnetization along [001] (black lines) and [111] (blue or gray lines). Top inset shows crystallographic axes relevant to the measurement, where the surface plane is (100). Lower insets show expanded views of peaks A, B, E, and F in the XMCD, for $\theta = 0°$ ([001], solid squares), $\theta = 30°$ (open squares), $\theta = 55°$ ([111], solid circles), and $\theta = 70°$ (open circles).

background correction performed is the subtraction of a linear slope from the XAS spectra.

Figure 1 shows XAS and XMCD spectra for measurements along the out-of-plane [001] direction ($\theta = 0$) and along the [111] direction (at $\theta = 54.7°$ towards the [110] direction) for an annealed 50 nm thick (Ga,Mn)As sample with $T_C = 145$ K and Mn concentration $x = 0.084$. The sample temperature is 6 K, the external magnetic field is ± 2 T (high enough to overcome any anisotropy field within the sample), and the x-ray polarization is $99 \pm 1\%$ circular. A remarkable difference is observed between the two measurements in both XAS and XMCD. The anisotropy of the XMCD features is most pronounced at the peaks labeled C and F, where the intensity increases by around 65% and 45%, respectively, on rotating the measurement axis from [111] to [001] and at peak E, where a change of sign of the XMCD is observed. There is also a significant anisotropy in the preedge features A and B, expanded in the left inset of Fig. 1(b). A similar angle dependence of the XAS and XMCD spectra is observed in other (Ga,Mn)As films studied. The anisotropy is largest in samples which show a large XMCD signal (i.e., where the magnetic moment per Mn atom is large) and disappears above T_C.

Figures 2(a)–2(c) show the intensity of the features labeled A, B, and C in Fig. 1 as a function of θ, for rotation towards either the [110] ($\phi = 45°$) or the [010] ($\phi = 0$) in-plane axes. Peaks A and C show a cubic symmetry about the ⟨100⟩ crystalline axes: for $\phi = 0$, the peak intensity is symmetric about $\theta = 45°$, corresponding to the [011] axis, while for $\phi = 45°$, the largest anisotropy is observed between $\theta = 0$ and $\theta = 54.7°$, i.e., the [001] and [111] axes. This cubic symmetry is emphasized by the dashed lines in Fig. 2 corresponding to the lowest order term in the expression for the cubic anisotropy $a_0 + a_1(\sin^4\theta \sin^2 2\phi + \sin^2 2\theta)$. This gives good agreement with the experimental result for peaks A and C for both planes. Note that the values of the coefficients a_0 and a_1 are energy dependent; i.e., they can be different for each specific peak. The same cubic symmetry is observed for the peaks E and F marked in Fig. 1(b). On the other hand, for peak B the XMCD increases monotonically on going from out-of-plane to in-plane magnetization in both (100) and (110) planes, changing sign at $\theta \sim 55°$. The dashed line shows a fit to the uniaxial dependence $a_0 + a_1\cos^2\theta$. Therefore, peak B depends only on the polar angle with respect to the out-of-plane direction. In (Ga,Mn)As, the Mn predominantly occupies the Ga site in the zincblende lattice, with tetrahedral symmetry. However, (Ga, Mn)As/GaAs(001) is under compressive strain, which breaks the symmetry between in-plane and out-of-plane directions [1]. Thus, while peaks A, C, E, and F share the cubic symmetry of the Mn site, peak B reflects the uniaxial symmetry of the strain field.

The compressive strain in (Ga, Mn)As/GaAs(001) has a marked influence on the magnetic anisotropy. In general, (Ga,Mn)As has a cubic magnetic anisotropy favoring mag-

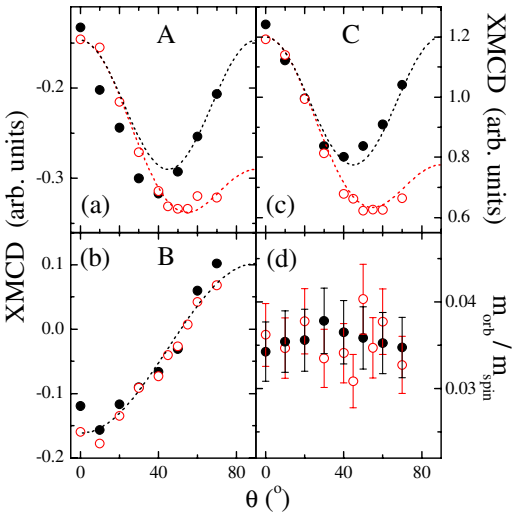

FIG. 2 (color online). (a)–(c) Dependence of the XMCD signal on the polar angle θ at the peak positions A, B, and C as marked in Fig. 1. Dashed lines are fits to the lowest order term in the anisotropy; (d) ratio m_{orb}/m_{spin} as obtained from the XMCD sum rules, versus θ, for azimuthal angle $\phi = 45°$ [(110) plane, open circles] and for $\phi = 0$ [(100) plane, solid circles].

netization along the ⟨100⟩ crystalline axes. However, strain leads to a large uniaxial magnetic anisotropy, favoring magnetization in plane for compressive strained films and out of plane for tensile strain [6,24]. This uniaxial anisotropy field is ~60 k Oe for the film reported in Figs. 1 and 2, which is around an order of magnitude larger than the shape anisotropy. In metal films (e.g., Co/Au [20]) a clear correspondence between magnetocrystalline anisotropy and anisotropy in m_{orb} has been demonstrated, with maximal m_{orb} along the easy magnetic axis. This suggests that the observed anisotropies in individual features in the XMCD spectrum of (Ga,Mn)As may be related to the cubic and uniaxial magnetic anisotropies. However, the integrated XMCD over both L_2 and L_3 edges, which is proportional to m_{orb} according to the XMCD sum rule [17], is found to be isotropic within the experimental uncertainty. Figure 2(d) shows m_{orb}/m_{spin} obtained from the Mn $L_{2,3}$ XMCD using the sum rules applied according to the procedure described in Ref. [13]. The obtained m_{spin}, m_{orb}, and m_{orb}/m_{spin} are, respectively, $4.3 \pm 0.3\mu_B$, $0.15 \pm 0.03\mu_B$, and 0.035 ± 0.005, independent of θ ϕ. The absence of a significant anisotropy in the magnetic moments indicates that the Mn 3d states do not contribute significantly to the magnetic anisotropy. This is consistent with the p-d Zener description of ferromagnetism in (Ga,Mn)As, in which large magnetic anisotropies can arise due to the splitting by strain of the host valence bands with As 4p character [7]. It should be noted that a net anisotropy on integrating over the uniaxially anisotropic preedge peak is not ruled out, but is within the experimental uncertainty due to the small size of this feature compared to the rest of the spectrum.

Figure 3 shows atomic multiplet calculations [25] for a d^5 configuration in tetrahedral crystal field of $10Dq = -0.5$ eV, for magnetization along the ⟨100⟩ and ⟨111⟩ axes. The calculation qualitatively reproduces most of the multiplet structure of the Mn $L_{2,3}$ XMCD and correctly predicts the anisotropy of each feature. The agreement with experiment is significantly better than recent density-functional calculations for various configurations of substitutional and interstitial Mn [14,15]. This is in spite of the simplicity of the atomic model, in which the detailed band structure of Mn in GaAs is not taken into account. The cubic anisotropy of the XMCD spectra is thus a single-ion property and does not rely on the orientation dependence of p-d hybridization which has been predicted for Mn in GaAs [8]. It should therefore be a generic phenomenon for localized or weakly metallic ferromagnetic systems. We can attribute these atomiclike features with cubic symmetry to transitions to localized unoccupied minority-spin states which lie well above E_F [8,9]. However, the calculated spectra only show a single peak in the preedge region. Peak B in the experimental spectrum is not reproduced by the atomic d^5 calculation, so must be of a different origin.

Figures 4(a) and 4(b) show XMCD spectra for five different (Ga,Mn)As films at $\theta = 0$. The spectra are normalized at the Mn L_3 XMCD peak. Most of the multiplet structure is independent of the Mn concentration, x, as reported previously [14]. In contrast, peak B shows a marked sample dependence, going from positive (i.e., opposite sign to the main L_3 peak) to negative sign on low-temperature annealing, and becoming more negative with increasing x. The inset of Fig. 4(a) shows the size of peak B versus the hole concentration, p, obtained from Hall measurements at 0.3 K and 16 T on samples with the same x and T_C. A clear correlation can be observed, with peak B

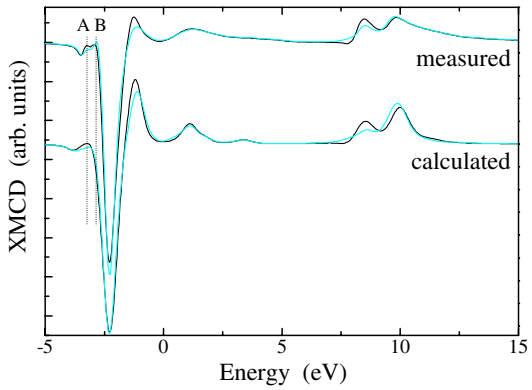

FIG. 3 (color online). Measured Mn $L_{2,3}$ XMCD for (Ga,Mn)As (upper curves) and calculated spectra for Mn d^5 configuration in tetrahedral crystal field of $10Dq = -0.5$ eV (lower curves), with magnetization along ⟨001⟩ (black lines) and along ⟨111⟩ (blue or gray lines). The vertical lines mark the positions of the preedge peaks A and B.

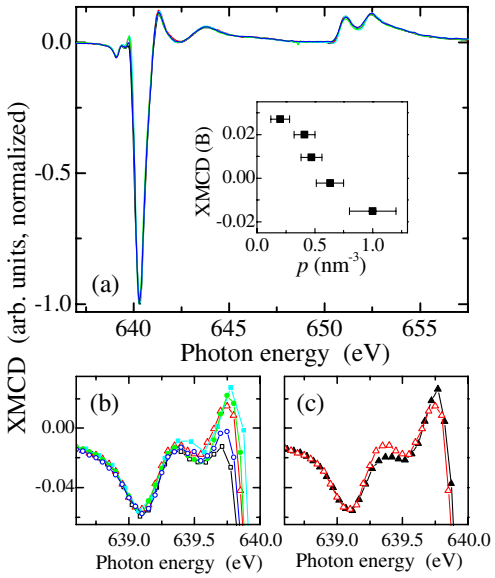

FIG. 4 (color online). (a),(b) Mn $L_{2,3}$ XMCD spectra at $\theta = 0$ for (Ga,Mn)As films with $x = 0.084$ annealed (open squares), $x = 0.034$ annealed (open circles), $x = 0.022$ annealed (open triangles), $x = 0.034$ as grown (solid circles), $x = 0.084$ as grown (solid squares). (c) XMCD preedge structure for annealed $x = 0.022$ (Ga,Mn)As at $\theta = 0$ (open triangles) and $\theta = 60°$ (solid triangles). The inset of (a) shows the hole density dependence of the XMCD at peak B.

becoming monotonically more negative with increasing p. The intensity of peak B is thus dependent on the Fermi level position, indicating that this feature corresponds to transitions to states at or just above E_F. For all five samples, the uniaxial anisotropy of peak B is observed, with an increase towards positive values on moving towards $\theta = 90°$, as shown in Fig. 4(c) for the annealed $x = 0.022$ film.

It is known that Mn can occupy both substitutional and interstitial sites in (Ga,Mn)As [2]. Therefore, it is tempting to attribute peak B to interstitial Mn. We rule this out because of the following: (i) the interstitial concentration should be similarly small in the three annealed samples presented in Fig. 4, while the size of peak B is quite different; (ii) interstitial Mn ions in (Ga,Mn)As are not ferromagnetic according to model calculations [26], so should not contribute to the XMCD. Instead, the uniaxial anisotropy and the correlation with hole density indicate that peak B is due to hybridization of Mn d states with strain-split GaAs valence states at E_F. Recent self-interaction corrected density-functional calculations indicate that a weak tail of majority spin d states extend to above E_F [9]. This overlap with valence band holes is essential for the large p-d exchange coupling which underpins ferromagnetism in (Ga,Mn)As [8]. The present results are clear evidence of a small, but finite, density of unoccupied Mn d states lying close to E_F.

In summary, we have resolved features with cubic and uniaxial anisotropy in the Mn $L_{2,3}$ XMCD spectra from (Ga,Mn)As. These are attributed, respectively, to localized atomiclike states lying far above E_F and states which are strongly hybridized with the valence bands of the GaAs host. Thus, both localized and hybridized Mn $3d$ states are observed in this system. No net anisotropy of the Mn $3d$ magnetic moments is observed. The ability to separately resolve localized and hybridized d states makes angle-dependent XMCD a powerful method for determining the electronic structure of magnetic semiconductors.

We thank Julio Cezar, Peter Bencok, and Nicholas Brookes for assistance with the measurements at ESRF, and Tomas Jungwirth, Kaiyou Wang, and Maciej Sawicki for valuable discussions. This work was supported by the U.K. EPSRC, CCLRC and Royal Society, and U.S. DOE.

[1] H. Ohno, A. Shen, F. Matsukura, A. Oiwa, A. Endo, S. Katsumoto, and Y. Iye, Appl. Phys. Lett. **69**, 363 (1996).

[2] K. M. Yu, W. Walukiewicz, T. Wojtowicz, I. Kuryliszyn, X. Liu, Y. Sasaki, and J. K. Furdyna, Phys. Rev. B **65**, 201303 (2002).

[3] K. W. Edmonds, P. Bogusławski, K. Y. Wang, R. P. Campion, S. N. Novikov, N. R. S. Farley, B. L. Gallagher, C. T. Foxon, M. Sawicki, T. Dietl, M. Buongiorno Nardelli, and J. Bernholc, Phys. Rev. Lett. **92**, 037201 (2004).

[4] T. Jungwirth, K. Y. Wang, J. Mašek, K. W. Edmonds, J. König, J. Sinova, M. Polini, N. A. Goncharuk, A. H. MacDonald, M. Sawicki, A. W. Rushforth, R. P. Campion, L. X. Zhao, C. T. Foxon, and B. L. Gallagher, Phys. Rev. B **72**, 165204 (2005).

[5] U. Welp, V. K. Vlasko-Vlasov, X. Liu, J. K. Furdyna, and T. Wojtowicz, Phys. Rev. Lett. **90**, 167206 (2003).

[6] X. Liu, Y. Sasaki, and J. K. Furdyna, Phys. Rev. B **67**, 205204 (2003).

[7] T. Dietl, H. Ohno, and F. Matsukura, Phys. Rev. B **63**, 195205 (2001); M. Abolfath, T. Jungwirth, J. Brum, and A. H. MacDonald, Phys. Rev. B **63**, 054418 (2001).

[8] P. Mahadevan, A. Zunger, and D. D. Sarma, Phys. Rev. Lett. **93**, 177201 (2004).

[9] T. C. Schulthess, W. M. Temmerman, Z. Szotek, W. H. Butler, and G. M. Stocks, Nat. Mater. **4**, 838 (2005).

[10] H. Ohldag, V. Solinus, F. U. Hillebrecht, J. B. Goedkoep, M. Finazzi, F. Matsukura, and H. Ohno, Appl. Phys. Lett. **76**, 2928 (2000).

[11] Y. L. Soo, G. Kioseoglou, S. Kim, X. Chen, H. Luo, Y. H. Kao, H.-J. Lin, H. H. Hsieh, T. Y. Hou, C. T. Chen, Y. Sasaki, X. Liu, and J. K. Furdyna, Phys. Rev. B **67**, 214401 (2003).

[12] K. W. Edmonds, N. R. S. Farley, R. P. Campion, C. T. Foxon, B. L. Gallagher, T. K. Johal, G. van der Laan, M. MacKenzie, J. N. Chapman, and E. Arenholz, Appl. Phys. Lett. **84**, 4065 (2004).

[13] K. W. Edmonds, N. R. S. Farley, T. K. Johal, G. van der Laan, R. P. Campion, B. L. Gallagher, and C. T. Foxon, Phys. Rev. B **71**, 064418 (2005).

[14] D. Wu, D. J. Keavney, R. Wu, E. Johnston-Halperin, D. D. Awschalom, and J. Shi, Phys. Rev. B **71**, 153310 (2005).

[15] R. Wu, Phys. Rev. Lett. **94**, 207201 (2005).

[16] P. T. Chiu, B. W. Wessels, D. J. Keavney, and J. W. Freeland, Appl. Phys. Lett. **86**, 072505 (2005).

[17] B. T. Thole, P. Carra, F. Sette, and G. van der Laan, Phys. Rev. Lett. **68**, 1943 (1992).

[18] P. Carra, B. T. Thole, M. Altarelli, and X. Wang, Phys. Rev. Lett. **70**, 694 (1993).

[19] J. Stöhr and H. Konig, Phys. Rev. Lett. **75**, 3748 (1995).

[20] D. Weller, J. Stöhr, R. Nakajima, A. Carl, M. G. Samant, C. Chappert, R. Mégy, P. Beauvillain, P. Veillet, and G. A. Held, Phys. Rev. Lett. **75**, 3752 (1995); H. A. Dürr, G. van der Laan, and B. T. Thole, Phys. Rev. Lett. **76**, 3464 (1996).

[21] P. Bruno, Phys. Rev. B **39**, R865 (1989).

[22] G. van der Laan, J. Phys. Condens. Matter **10**, 3239 (1998).

[23] R. P. Campion, K. W. Edmonds, L. X. Zhao, K. Y. Wang, C. T. Foxon, B. L. Gallagher, and C. R. Staddon, J. Cryst. Growth **247**, 42 (2003).

[24] This anisotropy can be reversed in the case of very low hole densities: M. Sawicki, F. Matsukura, A. Idziaszek, T. Dietl, G. M. Schott, C. Rüster, C. Gould, G. Karczewski, G. Schmidt, and L. W. Molenkamp, Phys. Rev. B **70**, 245325(R) (2004).

[25] G. van der Laan and B. T. Thole, Phys. Rev. B **43**, 13 401 (1991).

[26] J. Blinowski and P. Kacman, Phys. Rev. B **67**, 121204(R) (2003).